

antenna within acceptable limits. Consequently, the proposed antenna can be considered to be a useful candidate for many wideband communication systems providing 89.1% impedance bandwidth with average gain of 6 dBi.

ACKNOWLEDGMENTS

One of the authors, D. R. Poddar is grateful to All India Council for Technical Education (AICTE) for awarding him “Emeritus Fellow” and supporting this research via grant no. 1-51 RID/EF/ (04)/2009-10, dated January 06, 2010. Rowdra Ghatak is grateful to Department of Science and Technology, Government of India for supporting the simulation using CST Microwave Studio™ procured under Young Scientist Scheme vide sanction no. SR/FTP/ETA-0033/2010, dated August 31, 2010 and also grateful to Department of Science and Technology, Government of India for supporting measurement using VNA procured under DST-FIST grant to ECE Department, NIT Durgapur vide sanction No. SR/FST/ETI-267/2012(c), dated June 10, 2011.

REFERENCES

1. Y.X. Guo, C.L. Mak, K.M. Luk, and K.F. Lee, Analysis and design of L-probe proximity fed patch antennas, *IEEE Trans Antennas Propag* 49 (2001), 145–149.
2. E. Nishiyama, M. Aikawa, and S. Egashira, Stacked microstrip antenna for wideband and high gain, *IEE Proc Microwave Antennas Propag* 151 (2004), 143–148.
3. S.D. Targonski, R.B. Waterhouse, and D.M. Pozar, Design of wideband aperture stacked patch microstrip antennas, *IEEE Trans Antennas Propag* 46 (1998), 1245–1251.
4. Nasimuddin and Z.N. Chen, Wideband multilayered microstrip antennas fed by coplanar waveguide-loop with and without via combinations, *IET Microwaves Antennas Propag* 3 (2009), 85–91.
5. R. Ghatak, R.K. Mishra, and D.R. Poddar, Stacked dual layer complementing Sierpinski gasket planar antenna, *Microwave Opt Technol Lett* 49 (2007), 2831–2833.
6. J. Maik and M.V. Kartikeyan, A stacked equilateral triangular patch antenna with Sierpinski gasket fractal for WLAN application, *Prog Electromagn Res Lett* 22 (2011), 71–81.
7. K.P. Ray, V. Sevani, and S. Kakatkar, Compact broadband gap-coupled rectangular microstrip antennas, *Microwave Opt Technol Lett* 48 (2006), 2384–2389.
8. H.L. Dholakiya and D.A. Pujara, Improving the bandwidth of a microstrip antenna with a circular-shaped fractal slot, *Microwave Opt Technol Lett* 55 (2013), 786–789.
9. K. Falconer, *Fractal geometry*, 2nd ed.
10. Y. Lee, J. Yeo, R. Mitra, S. Ganguly, and J. Tenbarger, Fractal and multiband communication antennas, In: *IEEE Topical Conference on Wireless Communication Technology*, Honolulu, Hawaii, 2003, pp. 273–274.
11. Y. Mushiak, Self-complementary antennas, *IEEE Trans Antennas Propag* 34 (1992), 23–29.
12. B.L. Ooi, E.S. Siah, and P.S. Kooi, A novel microstrip fed slot – Coupled self complementary patch antenna, *Microwave Opt Technol Lett* 23 (1999), 284–289.
13. K.M. Luk, K.F. Lee, and Y.L. Chow, Proximity-coupled stacked circular-disc microstrip antenna with slots, *Electron Lett* 34 (1998), 419–420.
14. C.A. Balanis, *Antenna theory*, Wiley, Hoboken, NJ, 3rd ed.
15. G. Kumar and K.P. Ray, *Broadband microstrip antennas*, Artech House, Norwood, MA.
16. C. Borja and J. Romeu, On the behavior of the Koch island fractal boundary microstrip patch antenna, *IEEE Trans Antennas Propag* 51 (2003), 1281–1291.

COMPACT LOWPASS FILTER WITH HIGH OUT-OF-BAND REJECTION AND SUPERWIDE STOPBAND PERFORMANCE

Milad Mirzaee¹ and Bal S. Virdee²

¹Department of Electrical Engineering, Islamic Azad University, Eslamabad-E-Gharb Branch, Kermanshah, Iran; Corresponding author: milad.mirzaee@gmail.com

²Faculty of Life Sciences and Computing, Centre for Communications Technology, London Metropolitan University, London, United Kingdom

Received 24 July 2013

ABSTRACT: Presented is a novel design approach using multiple stub-loaded tapered microstrip resonator cells to create a compact lowpass filter with excellent in-band and out-of-band performance. The proposed structure achieves size reduction of greater than 50% and stopband enhancement of 245% in comparison with classical design. The new filter topology exhibits less than 0.5-dB passband loss, better than 15-dB return loss, and superwide stopband with rejection better than 40 dB up to 50 GHz. © 2014 Wiley Periodicals, Inc. *Microwave Opt Technol Lett* 56:947–950, 2014; View this article online at wileyonlinelibrary.com. DOI 10.1002/mop.28209

Key words: lowpass filter; tapered microstrip resonator cell; high rejection; superwide stopband

1. INTRODUCTION

Filters provide vital frequency control functions in a wide range of RF/microwave systems, especially when a variety of different communications systems are colocated or in close proximity to each other. Nowadays, such systems must adapt to an increasingly complicated electromagnetic (EM) environment and satisfy stringent requirements for applications in carrier-based, airborne,

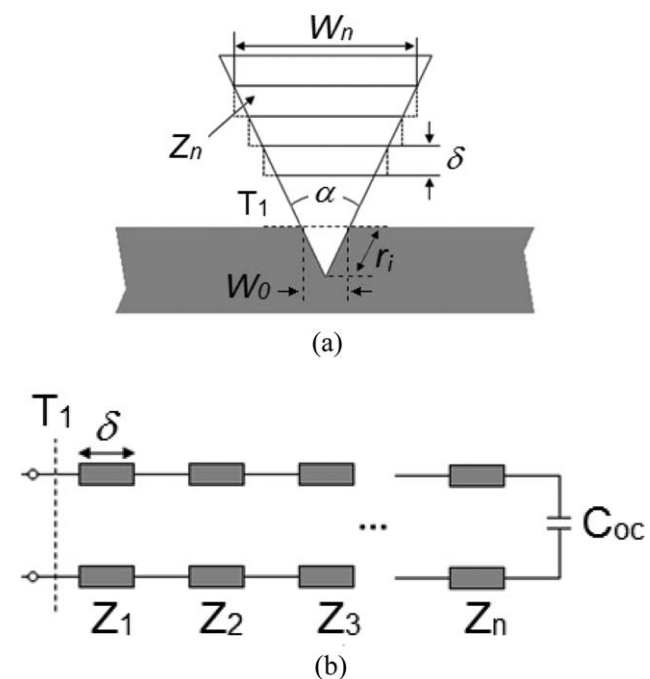


Figure 1 (a) Geometry of single delta-stub loading and (b) equivalent circuit model

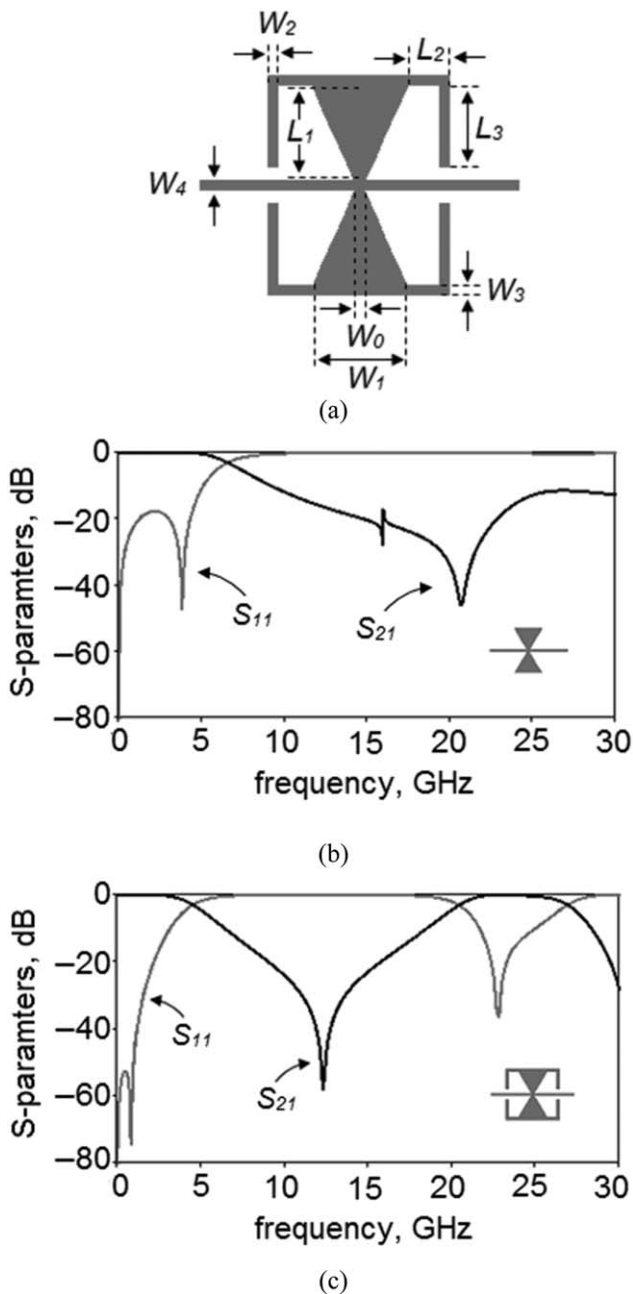


Figure 2 (a) Layout of the proposed resonator, where the optimized parameters are: $l_1 = 2$, $l_2 = 1.4$, $l_3 = 1.7$, $w_0 = 0.2$, $w_1 = 2$, $w_2 = 0.2$, $w_3 = 0.2$, and $w_4 = 0.2$ (all in mm), (b) simulated S -parameters of the proposed resonator without folded open stubs, and (c) simulated S -parameters of the proposed resonator with folded open stubs

and space environments. Lowpass filters (LPF) designed for use in wireless microwave communications systems must feature a low passband insertion loss, sharp roll-off, and wide rejection bandwidth. They have taken on many different forms and use a variety of design techniques which can be classified in three general groups, namely: (i) designs based on periodic arrangement of microstrip resonator cells [1, 2], (ii) designs based on symmetrically loaded resonant microstrip patches that are interconnected to each other through high impedance transmission lines [3, 4], and (iii) designs using defected ground structure[5, 6]. The main shortcomings of these approaches are: (i) limited passband, (ii) limited stopband, and (iii) relatively large circuit

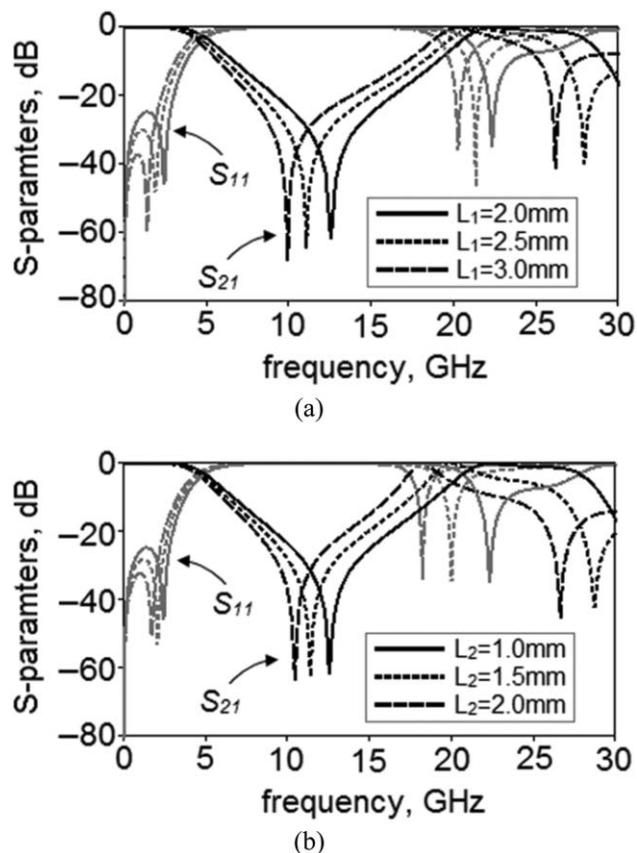


Figure 3 (a) Controlling transmission zero by changing the L_1 and (b) controlling transmission zero by changing the L_2

size. These features render such designs unsuitable for applications requiring an extended passband and stopband performance. An improved design was reported in [7, 8] using a topology consisting of semicircle and semiellipse loaded delta-shaped resonator and tapered resonators respectively. Although a compact filter is realized that exhibits a wider passband and stopband, these designs fall short of applications extending to millimetric waves.

In this article, we have developed a new compact lowpass filter that has low passband loss, a very sharp cutoff response, and superwide stopband up to 60 GHz. This was achieved using cascaded multiple stub-loaded tapered microstrip resonator cells (TMRCs). In comparison to the LPF in [7], size reduction of more than 50% and stopband enhancement of 245% are achieved.

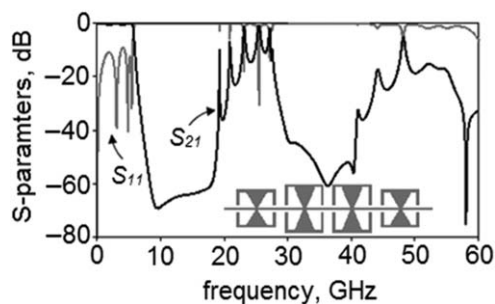


Figure 4 Simulated S -parameters of the proposed structure without using open stubs at the input/output

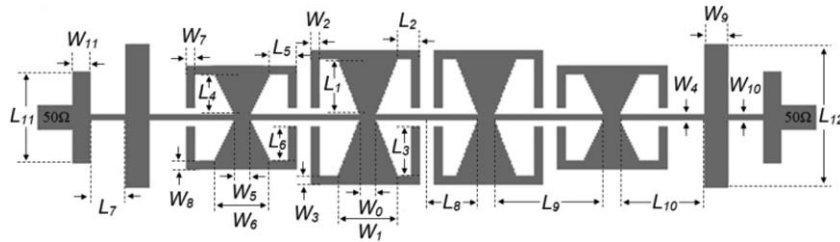


Figure 5 Layout of the proposed filter, where the optimized parameters are: $l_1 = 2$, $l_2 = 1$, $l_3 = 1.7$, $l_4 = 1.5$, $l_5 = 1$, $l_6 = 1.2$, $l_7 = 1.2$, $l_8 = 2.1$, $l_9 = 4.2$, $l_{10} = 3.2$, $l_{11} = 5$, $l_{12} = 3.2$, $w_0 = 0.2$, $w_1 = 2$, $w_2 = 0.2$, $w_3 = 0.2$, $w_4 = 0.2$, $w_5 = 0.2$, $w_6 = 2$, $w_7 = 0.2$, $w_8 = 0.2$, $w_9 = 0.8$, $w_{10} = 0.2$, and $w_{11} = 0.5$ (all in mm)

2. FILTER STRUCTURE

The resonator configuration comprises of a horizontal signal path which is tapped by two identical delta-stubs on either side of the path. The delta-stub and its equivalent circuit model are shown in Figure 1. The open end of the delta-stub is transformed to a short circuit at the plane T_1 , indicated in Figures 1(a) and 1(b). To achieve better performance, the delta-stubs are symmetrically loaded with folded open-circuit stubs, as shown in Figure 2(a).

The delta-stub tapered line is modeled by a series of n transmission line segments of thickness δ [9]. The value of n is chosen so that each segment is $\ll \lambda_g$ [10]. The characteristic impedance of each segment is determined using the standard microstrip line equations with the exception of the final segment, which has an open-end discontinuity [10]. Widths of segments can be calculated using

$$W = 2n\delta \tan \frac{\alpha}{2} \quad (n = 0, 1, 2, \dots) \quad (1)$$

where α is the vertex angle of the delta-stub indicated in Figure 1(a). When $W/h \geq 1$ (h is a thickness of substrate), the characteristic impedance of each segment can be calculated using

$$Z_0 = \frac{120\pi}{\sqrt{\epsilon_e} [w/h + 1.393 + 0.667 \ln(w/h + 1.444)]} \quad (2)$$

where ϵ_e is the effective dielectric constant of a microstrip line. The relation between the width of the feed-line W_0 and inner radius r_1 of the delta-stub is given by

$$W_0 = 2r_1 \sin \frac{\alpha}{2}. \quad (3)$$

Delta-stub is capable of yielding a wider bandwidth and due to its straight sides it may be easier to lay out on PCB than radial stub. Figure 2(a) shows the geometry of the proposed resonator and its characterizing structural parameters. It should be noted that loading the delta-stubs with folded open-circuit stubs does result in a lower cutoff frequency and consequently, steeper descent of the transition from passband-to-stopband as depicted in Figures 2(b) and 2(c). The main reason for this behavior is that the increase in the series inductance results in a decrease in the resonant frequency of the proposed resonator. Several degrees of freedom exist for adjusting the frequency response of the proposed resonator. A transmission zero can be observed near the passband edge at 12.19 GHz, but its location and rejection level can be adjusted by changing the size of L_1 and L_2 . As can be seen in Figures 3(a) and 3(b), when either L_1 or L_2 are increased, while the other parameters remain fixed, the transmission zero at 12.19 GHz will decrease in frequency. The location of the transmission zero and consequently, the sharpness of the transition from passband-to-stopband can be controlled by varying L_1 and L_2 . Although the simulation results

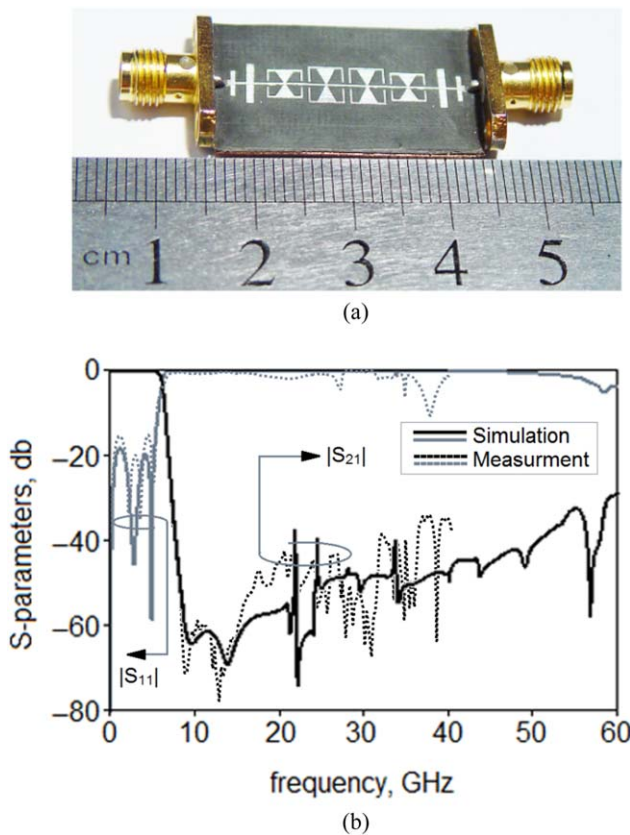


Figure 6 (a) Photograph of the fabricated filter and (b) measured (dashed line) and simulated S -parameters (solid line) of the proposed lowpass filter. [Color figure can be viewed in the online issue, which is available at wileyonlinelibrary.com]

TABLE 1 Comparison Between Current Design and Previous Works

Reference	Size (mm ²)	Cutoff (GHz)	IL/RL (dB)	Stopband up to (GHz) for Rejection Level
[1]	641.33	1.30	<1.0/19.5	13.0 for > -20 dB
[2]	500.98	1.33	<1.0/10.0	2.15 for > -45 dB
[3]	271.18	1.00	0.40/<15	20.0 for > -15 dB
[4]	265.20	0.85	0.36/<15	12.6 for > -25 dB
[5]	1156.0	2.62	<1.0/25.0	14.0 for > -26 dB
[6]	174.00	3.70	<0.5/<10	7.50 for > -20 dB
[7]	250.36	3.12	0.33/11.3	19.0 for > -20 dB
[8]	110.89	3.00	0.03/20.0	20.0 for > -25 dB
This work	124.00	6.00	<0.5/<15	60.0 for > -29 dB

indicate an acceptable lowpass filter response, the filter design falls short of some requirements, notably in the transition and stopband regions. The filter's roll-off response and out-of-band rejection were significantly improved by cascading several resonators together. To cancel unwanted spurious demonstrated in Figure 4 and, therefore, expand the filter's rejection bandwidth, open-circuit stubs capable of providing transmission zeros were used in conjunction with the multiple stub-loaded TMRCs. The structure of the final filter is shown in Figure 5.

3. FABRICATION AND MEASUREMENT

Simulations on the performance of the lowpass filter design were performed by means of EM simulation using the Advanced Design System. The filter was designed and fabricated on RT/duroid 5880 circuit material with relative permittivity of 2.2, thickness of 10 mils, and loss tangent of 0.0009. The filter's S -parameters were measured using Agilent 8722ES network analyzer. A photograph of the fabricated filter is shown in Figure 6(a). Its simulated and measured S -parameters responses are given in Figure 6(b). The results show that the proposed filter has a 3-dB cutoff frequency of 6 GHz and insertion loss of less than 0.5 dB throughout the passband. The return loss is better than 15 dB in this region. The stopband return loss demonstrates that this filter possesses low radiation loss. The filter design is shown to provide a stopband extending up to 60 GHz with suppression better than -40 dB up to 50 GHz, and 158% relative stopband bandwidth. Compared to other lowpass filter designs reported to date, see Table 1, the proposed filter offers superior performance in terms of size, passband insertion loss and return loss, and stopband bandwidth and stopband rejection levels.

It should be noted that the authors in [7] have used the delta-stub as a basic resonator as well. In comparison to the UWB filter in [7], the proposed filter has 92% increase in passband, 245% increase in stopband, and more than 50% decrease in circuit area.

4. CONCLUSION

The feasibility of a highly compact lowpass filter has been experimentally demonstrated that exhibits a very steep 3-dB roll-off and superwide rejection bandwidth up to millimetric waves. The filter exhibits outstanding electrical performance, with passband loss of less than 0.5 dB, passband return loss better than 15 dB, and wide stopband with rejection better than 40 dB up to 50 GHz.

REFERENCES

1. L. Li, Z.-F. Li, and W.-F. Wei, Compact and selective lowpass filter with very wide stopband using tapered compact microstrip resonant cells, *Electron Lett* 45 (2009), 267–268.
2. F. Aznar, A. Velez, J. Bonache, J. Martel, and F. Martin, Compact lowpass filters with very sharp transition bands based on open complementary split ring resonators, *Electron Lett* 45 (2010), 316–317.
3. J. Wang, H. Cui, and G. Zhang, Design of compact microstrip lowpass filter with ultra-wide stopband, *Electron Lett* 48 (2012), 854–856.
4. H. Cui, J. Wang, and G. Zhang, Design of microstrip lowpass filter with compact size and ultra-wide stopband, *Electron Lett* 48 (2012), 856–857.
5. A.S. Mohra, Microstrip low pass filter with wideband rejection using opened circuit stubs and z-slots defected ground structures, *Microwave Opt Technol Lett* 53 (2011), 811–815.
6. Y. Yang, X. Zhu, and N.C. Karmakar, Microstrip lowpass filter based on split ring and complementary split ring resonators, *Microwave Opt Technol Lett* 54 (2012), 1723–1726.
7. M. Hayati, A. Sheikhi, and A. Lotfi, Compact lowpass filter with wide stopband using modified semi-elliptic and semi-circular microstrip patch resonator, *Electron Lett* 46 (2010), 1507–1509.

8. M. Mirzaee, B. Virdee, Realisation of highly compact planar lowpass filter for UWB RFID applications, *Electron. Lett.* 49 (2013), pp. 1396–1398.
9. B. Zhou, H. Wang, and W.-X. Sheng, A modified UWB wilkinson power divider using delta stub, *Prog. Electromagn. Res. Lett.* (2010), pp. 49–55.
10. C.B. Wadell: 'Transmission line design handbook' (Artech House, Norwood, MA, 1991), pp. 304–305.

© 2014 Wiley Periodicals, Inc.

SINGLE-LAYER REFLECTARRAY WITH NOVEL ELEMENTS FOR WIDEBAND APPLICATIONS

Wei-Wei Wu, Shi-Wei Qu, and Xiang-Qian Zhang

School of Electronic Engineering, University of Electronic Science and Technology of China (UESTC), Chengdu 611731, China; Corresponding author: shiweiqu@uestc.edu.cn

Received 28 July 2013

ABSTRACT: A novel single-layer reflectarray element with three resonances, showing a linear phase curve and a large phase variation range over 800° is proposed for a broadband operation. Different size of elements are selected by using a simple guideline to achieve the required phase distribution in a given frequency band. Two offset-fed 10×10 reflectarrays with different scattering angles are designed. Simulations and measurements show the bandwidth of 28% for a 3-dB gain drop and 44% for -10 -dB side lobe level inspite of the large F/D of 2.1. © 2014 Wiley Periodicals, Inc. *Microwave Opt Technol Lett* 56:950–954, 2014; View this article online at wileyonlinelibrary.com. DOI 10.1002/mop.28208

Key words: reflectarray; wideband antenna; antenna array

1. INTRODUCTION

Microstrip reflectarrays are rapidly becoming an attractive alternative to traditional parabolic reflectors and phased array antennas due to its various advantages such as surface mountable with low mass and small volume, low manufacturing cost [1], and significant simplification of feed systems relative to complex antenna systems as discussed in [2]. A printed reflectarray is a reflector composed of a planar array of microstrip elements on a grounded substrate. The size of the cell elements are adjusted to shape or collimate the radiated beam when illuminated by a feed horn as primary source. Although researches on reflectarrays began in the 1960's, improvements on the bandwidth are still being one of the most attractive tasks in recent years. The bandwidth of microstrip reflectarrays is dominated by two factors. The first one is the inherent narrow-band behavior of microstrip elements themselves. The second is different spatial phase delays resulting from different ray lengths from the feed to each point on the wave front of the radiated beam. For a medium-sized reflectarray, the former factor is more significant [3].

Elements with a linear phase response can be used to improve the array bandwidth [4]. Several methods were introduced to linearize the phase response, such as multilayer configurations [5], phase-delay lines [6], multiresonance dipoles [7], and multicross loop reflectarray [8]. However, multilayer configurations are very costly and often lead to serious surface waves. The phase range is as important as the linearity of the phase response. Although the three-resonance dipoles can achieve almost 1000° phase range, its nonlinear phase curve will